


Cite this: *RSC Adv.*, 2021, 11, 33425

# One-pot self-assembly preparation of thiol-functionalized poly(3,4-ethylenedioxythiophene) hollow nanosphere/Au composites, and their electrocatalytic properties†

Ahmat Ali, <sup>a</sup> Ruxangul Jamal<sup>b</sup> and Tursun Abdiryim <sup>\*b</sup>

In this work, we developed a thiol-functionalized poly(3,4-ethylenedioxythiophene) hollow sphere (poly(EDOT-MeSH)/Au) polymer through a simple one-pot self-assembly method using polyvinylpyrrolidone (PVP) as a soft template. The monomer was used as both a reductant and a stabilizer to decorate gold nanoparticles (Au NPs). FTIR, XRD, EDX, SEM and TEM analyses were used to characterize the composite hollow spheres. The chemical bond between S and Au was confirmed by XPS. The electrochemical performance of the composite hollow spheres was determined by cyclic voltammetry (CV) and an amperometric response timing current test. The results revealed that the poly(EDOT-MeSH)/Au hollow-sphere-based electrochemical sensor possesses excellent conductivity and high redox reversibility with detection limits ( $S/N = 3$ ) of 0.2, 0.02, 0.08 and 0.05  $\mu\text{M}$  in the linear ranges of 0.1–650  $\mu\text{M}$ , 0.05–100  $\mu\text{M}$  and 0.1–600  $\mu\text{M}$  for the determination of ascorbic acid (AA), dopamine (DA), uric acid (UA) and nitrate ions ( $\text{NO}_2^-$ ), respectively. The preparation method for these composites will further the development of this type of conducting polymer/gold nano-composite material modified electrochemical sensor for biological species.

Received 7th September 2021  
Accepted 29th September 2021

DOI: 10.1039/d1ra06732j

rsc.li/rsc-advances

## 1. Introduction

Polymer hollow nanospheres have attracted attention in various fields due to their high dispersibility in water systems and their easy loading onto the surface of nanoparticles: for example, heterogeneous catalysis, separation and protection of enzymes and proteins, and limiting reaction vessels.<sup>1</sup> Conducting polymer hollow nanospheres exhibit unique properties compared to conventional polymers, such as electron, optical, electrochemical, and redox reversibility.<sup>2,3</sup> The preparation method of the conducting polymer hollow nanosphere comprises coating with a layer of a polymer a hard template surface, such as silicon dioxide, nano inorganic particles or polystyrene spheres, and then removing the core by calcination, solvent etching, or polyvinylpyrrolidone (PVP), to produce a self-assembled soft template under the action of a surfactant such as cetyltrimethylammonium bromide (CTAB).<sup>4,5</sup> At present, most studies on conducting polymer hollow spheres are mainly limited to polyaniline and polypyrrole, while research on

PEDOT derivatives focuses on the preparation of needles, fibers and tubes.<sup>6,7</sup> It is reported that commonly used surfactants, such as PVP, CTAB and sodium dodecyl sulfate (SDS), can not only reduce the oxidation potential of EDOT, but also improve its solubility in aqueous solution and improve the interface interactions between the electrode and the solvent.<sup>8</sup> Dispersed solutions of PEDOT and PVP play an extremely important role in the preparation of electrochemical biosensors for PEDOT.<sup>9</sup> In addition, surfactants with a relatively large hydrophobic tail are capable of forming aggregated micelles in an aqueous system. PEDOT/inorganic nanomaterial composites combine the advantages of organic and inorganic phases. On the one hand, inorganic nanomaterials can adjust the aggregation morphology, improve carrier transport mobility and increase surface area. On the other hand, PEDOT contributes to the uniform loading of inorganic nanomaterials and improves the electrical conductivity and chemical stability of nanomaterials.<sup>10</sup> Specifically, metal nanoparticles such as Ag, Au, and Pd can be relatively easily supported on the surface of the PEDOT nanomaterial without any dispersant or reducing agent. Since Au NPs have a high affinity for sulfur atoms in the thiophene ring, it is easy to prepare composites of Au NPs and PEDOT.<sup>11</sup> In previous work, we prepared poly(EDOT-MeSH) hollow nanosphere/Au composites using  $\text{SiO}_2$  nanospheres as a hard template.<sup>12</sup> And we found that the thiol group on PEDOT effectively stabilizes the Au NPs and results in a uniform

<sup>a</sup>College of Chemistry and Environmental Engineering, Xinjiang Institute of Engineering, Urumqi 830023, Xinjiang Uygur Autonomous Region, China

<sup>b</sup>State Key Laboratory of Chemistry and Utilization of Carbon Based Energy Resources, Xinjiang University, Urumqi 830046, People's Republic of China. E-mail: tursunabdir@sina.com.cn

† Electronic supplementary information (ESI) available. See DOI: 10.1039/d1ra06732j





that the absorption peak at  $\sim 1090\text{ cm}^{-1}$  can be attributed to the vibrational peak of the PEDOT skeleton. The absorption peak at  $\sim 1655\text{ cm}^{-1}$  is the vibration peak of the doped PEDOT. Weak absorption peaks appeared at  $\sim 2870$  and  $\sim 2920\text{ cm}^{-1}$ , which are attributed to the stretching vibration peak of  $-\text{CH}_2$  in the dioxy-ethylene group. The absorption peaks at  $\sim 675$ ,  $760$ – $790$ , and  $920$ – $940\text{ cm}^{-1}$  are assigned to the vibrational peak of the  $-\text{C}-\text{S}-$  bond.<sup>11</sup> The absorption peak at  $920$ – $940\text{ cm}^{-1}$  is the vibration peak of the dioxy-ethylene deformation mode. Peaks at  $\sim 3115$ ,  $\sim 3010$  and  $\sim 2930\text{ cm}^{-1}$  are the deformation vibrations of  $\text{C}-\text{H}$ ,  $\text{C}-\text{H}-\text{C}$  and  $\text{C}-\text{H}_2-\text{C}$  on the long chain of the outer fatty acid. A relatively broad absorption peak appears at  $3200$ – $3700\text{ cm}^{-1}$  due to the vibrational peaks of  $\text{O}-\text{H}$  and  $\text{S}-\text{H}$ .<sup>13</sup> In addition, the FTIR spectra of the poly(EDOT-MeSH) and poly(EDOT-MeSH) hollow nanosphere/Au composites are very similar, due to there being no infrared absorption peaks in the infrared region for the Au nanoparticles. In addition, it can be seen from the FTIR spectrum of the poly(EDOT-MeSH) hollow nanosphere/Au composites that all of the absorption peaks are shifted to a low wave number. This result indicates that  $\text{HAuCl}_4$  acts as a relatively strong oxidant, giving the complex a higher degree of conjugation. In addition, the weaker absorption peak of  $675\text{ cm}^{-1}$  disappeared, while the vibration peak at  $3200$ – $3700\text{ cm}^{-1}$  was weakened. The reason may be that the Au NPs not only interact with the  $-\text{SH}$  of the alkyl chain in the composites, but also interact with S on the thiophene ring. The strong chemical interaction between S and Au may result in a weakening of the vibrational peak at  $3200$ – $3700\text{ cm}^{-1}$  and the disappearance of the absorption peak at  $675\text{ cm}^{-1}$ .

### 3.2 XRD spectra

The presence of Au NPs was confirmed from powder XRD patterns. As shown in Fig. 3, poly(EDOT-MeSH) exhibits a broad diffraction peak at  $2\theta = 20$ – $30^\circ$  due to the  $\pi$ - $\pi^*$  intermolecular stacking.<sup>14</sup> In the poly(EDOT-MeSH) hollow nanosphere/Au composites, diffraction peaks appear at  $2\theta = 38.20$ ,  $44.36^\circ$ ,

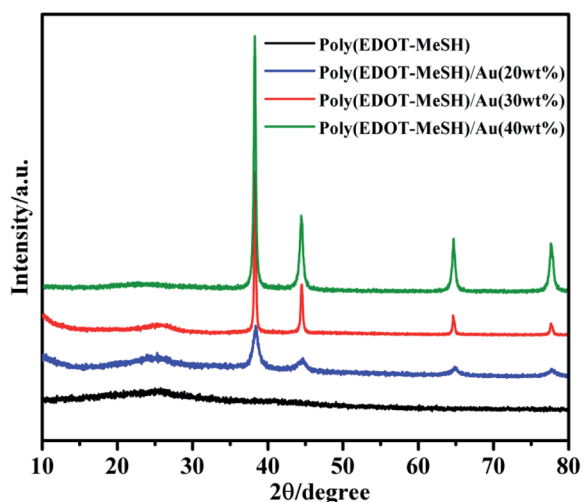


Fig. 3 XRD spectra of poly(EDOT-MeSH) and poly(EDOT-MeSH) hollow nanosphere/Au composites.

$64.75^\circ$  and  $77.60^\circ$ , as the content of  $\text{HAuCl}_4$  increases, which correspond to the (111), (200), (220) and (311) planes of Au NPs.<sup>15</sup> Moreover, the characteristic peak-to-peak intensity of the Au NPs increases with the addition of  $\text{HAuCl}_4$ . At the same time, the characteristic diffraction peak of poly(EDOT-MeSH) becomes sharper when the content of  $\text{HAuCl}_4$  is 30 wt%, and become weak at content of  $\text{HAuCl}_4$  up to 40%. The results show that the concentration of  $\text{HAuCl}_4$  in the reaction system affects the crystallinity of the polymer.

### 3.3 EDX spectra

Fig. S1† shows the EDX spectra of poly(EDOT-MeSH) hollow nanosphere/Au composites. Besides the C, S, O elements, the peak for the Au element also appeared, indicating that  $\text{HAuCl}_4$  has been successfully reduced to Au nanoparticles during the polymerization. As shown in Table 1, the contents of AuNPs were 6.05%, 14.69% and 30.2% for poly(EDOT-MeSH)/Au (20 wt%), poly(EDOT-MeSH)/Au (30 wt%) and poly(EDOT-MeSH)/Au (40 wt%) composites, respectively, indicating that there was a linear relationship between the amount of  $\text{HAuCl}_4$  and the content of AuNPs. However, there is no obvious linear relationship between the percentage of C element detected in the composites with different Au contents and the changes in other elements. This result may be due to the conductive paste and the environment which affected the percentage of C and O elements.

### 3.4 XPS spectra

To further investigate the chemical interaction between the S and Au elements, XPS analysis of the samples was performed.

Fig. 4 shows spectra of poly(EDOT-MeSH) and poly(EDOT-MeSH) hollow nanosphere/Au (30 wt%) composite. The full spectra shows peaks of 164, 285 and 532 eV, corresponding to the signals of O 1s, S 2p and C 1s, respectively. In addition, a peak of Au 4f appeared at 87 eV in the composite. The high-resolution XPS spectra of poly(EDOT-MeSH) and poly(EDOT-MeSH) hollow nanosphere/Au (30 wt%) composite are shown in Fig. 4(B–D). The results showed that the peaks of Au  $4f_{7/2}$  and Au  $4f_{5/2}$  appeared at 84.3 and 88 eV, indicating the presence of Au.<sup>16,17</sup>

Generally, the binding energies of the bulk Au 4f levels appeared at ( $4f_{7/2}$ ) 83.8 and ( $4f_{5/2}$ ) 87.6 eV, which suggested that there are chemical bonds between the Au atoms and S atoms in poly(EDOT-MeSH).<sup>18</sup>

In addition, the C 1s spectra of the polymers and composite show signal peaks for C–C, C–S and C–O bonds, which occur at 284.8, 286.1 and 288 eV, respectively (Fig. 4C). The S 2p spectra of poly(EDOT-MeSH) showed spin-split doublet peaks at 162.8

Table 1 The elemental compositions of the composites

Samples	C	O	S	Au
Poly(EDOTMeSH)/Au (20 wt%)	46.3	26.91	20.75	6.05
Poly(EDOTMeSH)/Au (30 wt%)	45.69	20.73	18.91	14.69
Poly(EDOTMeSH)/Au (30 wt%)	37.21	17.21	14.79	30.22





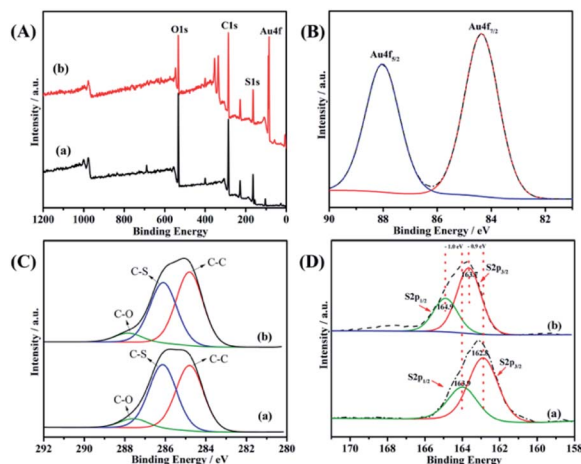


Fig. 4 XPS of poly(EDOT-MeSH) hollow nanosphere/Au (30 wt%) composite: (A) full spectra, (B) Au 4f spectra, (C) C 1s spectra, (D) S 2p spectra.

(S 2p<sub>3/2</sub>) and 163.9 eV (S 2p<sub>1/2</sub>), which correspond to unbound S atoms in the polymer.<sup>19</sup> For the poly(EDOT-MeSH) nanosphere/Au composites, the S 2p peaks appear at 163.7 (S 2p<sub>3/2</sub>) and 164.9 eV (S 2p<sub>1/2</sub>), which are 0.9 and 1.0 eV higher than that of the polymer. The results indicate that the enhancement in the S 2p bond energy should be caused by the chemical bond formed between Au and S.<sup>20,21</sup> Thus, it can be seen that the chemical bond between Au and S enables the Au nanoparticles to be better supported on the polymer surface and the matrix.

### 3.5 Morphology

Fig. 5 shows scanning electron microscopy (SEM) images of poly(EDOT-MeSH) and poly(EDOT-MeSH) hollow nanosphere/Au composites. The poly(EDOT-MeSH) hollow nanospheres exhibit a smooth spherical morphology with a diameter of 300–500 nm. In the poly(EDOT-MeSH) hollow nanosphere/Au composites, the composite obtained with 20 wt% HAuCl<sub>4</sub> shows a spherical shape of uniform size, but no Au

nanoparticles appear on the polymer surface. When HAuCl<sub>4</sub> is up to 30 wt%, uniform-sized Au NPs appear on the surface of the composite. When HAuCl<sub>4</sub> is 40 wt%, an irregular morphology appears, and the Au particles on the surface are also uneven in size, indicating that a high concentration of HAuCl<sub>4</sub> affects the morphology of the composite and the size of the Au NPs. It should be noted that in the polymerization process, the reaction system is carried out for 6 h with persulfuric acid as an oxidant, and then certain concentrations of HAuCl<sub>4</sub> are added slowly. The purpose is that forming spherical PVP-poly(EDOT-MeSH) oligomer through the self-assembly of PVP at the first step. And then, Au NPs grow together with the polymer through continues drop-wise addition of HAuCl<sub>4</sub>. As a strong oxidant, when the concentration of HAuCl<sub>4</sub> reaches a certain level, a polymerization reaction will occur in the system instead of the production of the PVP soft template.

Fig. 6 shows TEM images of poly(EDOT-MeSH) and poly(EDOT-MeSH) hollow nanosphere/Au composites. It can be seen from the figure that the polymer and composites show a spherical hollow structure. In addition, poly(EDOT-MeSH)/Au with different Au contents are composites of a spherical hollow polymer and Au NPs. In the SEM image, when the HAuCl<sub>4</sub> is 20 wt%, no Au NPs are found on the surface of the composite, while a small amount of Au NPs were observed in the TEM, indicating that most of the gold nanoparticles are well embedded in the polymer matrix instead of the polymer surface. As shown in Fig. 6(C and D), in poly(EDOT-MeSH)/Au (30 wt%), Au NPs are more uniformly dispersed than those of other composites. However, when HAuCl<sub>4</sub> is up to 40 wt%, poly(EDOT-MeSH)/Au almost loses its spherical structure, and the size of the formed Au NPs is not uniform, indicating that a high concentration of HAuCl<sub>4</sub> leads to the formation of a plate-like morphology.

Fig. 7 shows the HTEM of poly(EDOT-MeSH)/Au (30 wt%) and the particle size distribution of the nanoparticles. It is apparent from the figure that the Au NPs have a relatively small particle size with a relatively uniform dispersion. The average particle size of the Au NPs is obtained through statistical measurement of the particle size of 100 Au NPs. The particle size of Au nanoparticles in the poly(EDOT-MeSH) matrix is mainly in the range of 10.5–14.5 nm with an average particle size of 12.5 ± 0.5.

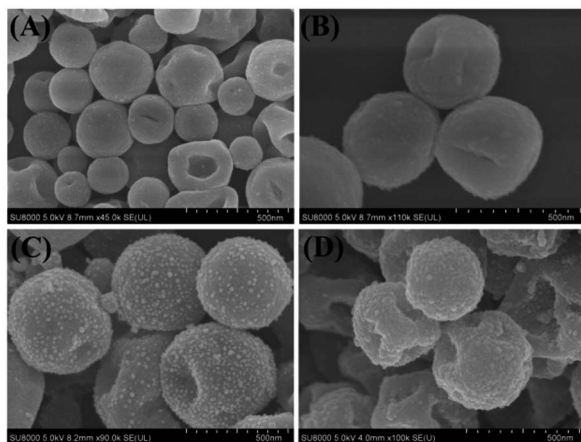


Fig. 5 SEM images of (A) poly(EDOT-MeSH), (B) poly(EDOT-MeSH)/Au (20 wt%), (C) poly(EDOT-MeSH)/Au (30 wt%), and (D) poly(EDOT-MeSH)/Au (40 wt%).

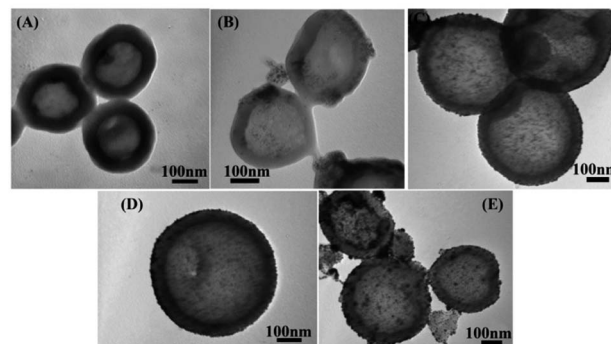


Fig. 6 TEM images of (A) poly(EDOT-MeSH), (B) poly(EDOT-MeSH)/Au (20 wt%), (C) and (D) poly(EDOT-MeSH)/Au (30 wt%), and (E) poly(EDOT-MeSH)/Au (40 wt%).



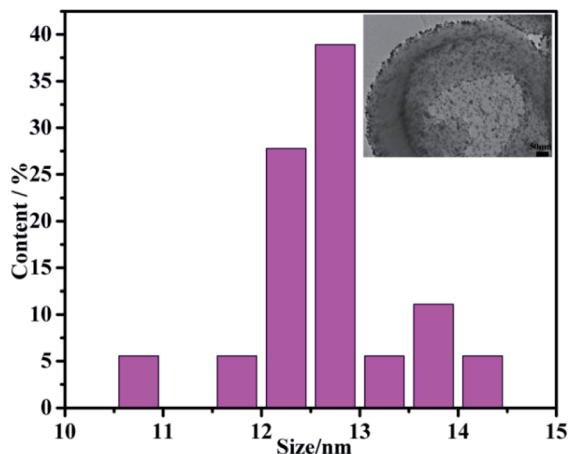


Fig. 7 Particle size distribution of the nanoparticles.

### 3.6 Electrochemical performance

In order to investigate the selectivity of the modified electrode, cyclic voltammetry was performed in 0.1 M PBS buffer solution containing 50  $\mu\text{M}$  DA, 200  $\mu\text{M}$  UA, and 150  $\mu\text{M}$   $\text{NO}_2^-$ . As shown in Fig. 8(B), when 50  $\mu\text{M}$  DA, 200  $\mu\text{M}$  UA, and 150  $\mu\text{M}$   $\text{NO}_2^-$  were added, the corresponding oxidation peaks of each substance appeared at 0.21, 0.35 and 0.92 V, respectively. This indicated that the poly(EDOT-MeSH)/Au (30 wt%) modified electrode shows catalytic activity toward DA, UA, and  $\text{NO}_2^-$ . In the cyclic voltammetry curve of the mixed system containing these three substances, the corresponding oxidation peaks of each substance can be observed, and the oxidation peak potential remains unchanged, indicating that the modified electrode can simultaneously detect these three substances. From the above experimental results, the poly(EDOT-MeSH)/Au (30 wt%) modified electrode has potential applications in the field of electrochemical sensors.

An amperometric response timing current test of the poly(EDOTMeSH)/Au (30 wt%) modified electrode for AA was conducted under the optimal experimental conditions. Fig. 9(A) shows the time-current curve for the continuous addition of AA (potential of 0.05 V), DA (potential of 0.25 V), UA (potential of 0.55 V),  $\text{NO}_2^-$  (potential of 0.89 V) in PBS buffer solution at the poly(EDOT-MeSH)/Au (30 wt%)/GCE, respectively. The oxidation current of the target species increased as the concentration increased.

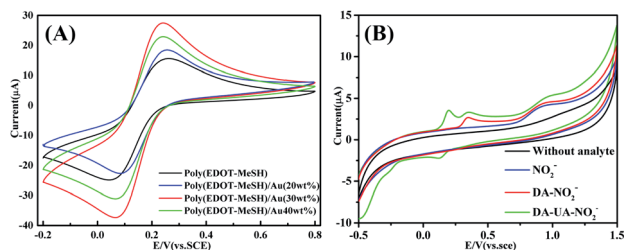


Fig. 8 CV of poly(EDOT-MeSH) and poly(EDOT-MeSH) hollow nanosphere/Au composites: (A) 5.0 mM  $[\text{Fe}(\text{CN})_6]^{3-/4-}/0.1 \text{ M KCl}$ , (B) 50  $\mu\text{M}$  DA, 200  $\mu\text{M}$  UA, 150  $\mu\text{M}$   $\text{NO}_2^-$ .

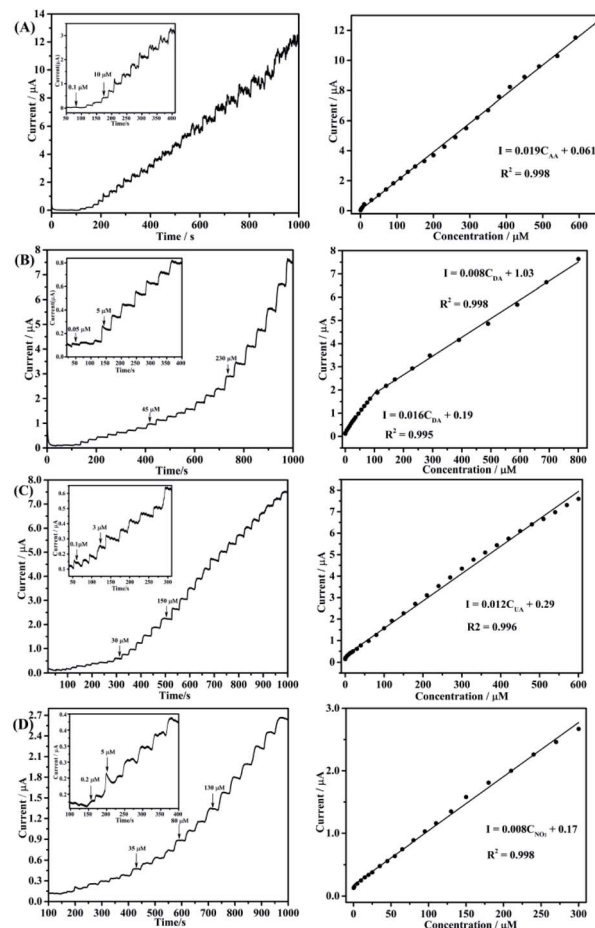


Fig. 9  $i-t$  curves (left) and corresponding relationship between concentration and peak current (right) of AA (A) DA (B), UA (C) and  $\text{NO}_2^-$  (D) in 0.1 M PBS buffer solution by the poly(EDOT-MeSH)/Au (30 wt%) modified electrode.

The corresponding detection ranges of AA, DA, UA and  $\text{NO}_2^-$  are 0.1–650  $\mu\text{M}$ , 0.05–100  $\mu\text{M}$ , 0.1–600  $\mu\text{M}$ , and 0.2–300  $\mu\text{M}$ , respectively. Corresponding detection limits calculated at  $\text{S/N} = 3$  are 0.2  $\mu\text{M}$ , 0.02  $\mu\text{M}$ , 0.08  $\mu\text{M}$ , and 0.05  $\mu\text{M}$ , respectively. The detailed results are shown in Table S1.† The high sensitivity and electron kinetics of the modified electrode can be deduced from the following aspects: at the first polymerization process for 6 h, oligomer and PVP micelles were achieved without  $\text{HAuCl}_4$ , at the same time avoiding the oligomerization of polymer and Au NPs. Second, in the polymerization process,  $\text{HAuCl}_4$  can be reduced to small-sized Au NPs by the EDOT-MeSH oligomer during the polymerization reaction. In this process, the  $-\text{SH}$  group acts as a stabilizer and functions as a bridge between poly(EDOT-MeSH) and the Au NPs, and this bridge---S-Au bond can bring about Au NPs uniformly imbedded in the outer and inner sides of the polymer.

### 3.7 Anti-interference performance test of modified electrode

As shown in Fig. 10, the anti-interference performance of the poly(EDOT-MeSH)/Au (30 wt%)GCE was tested. After each



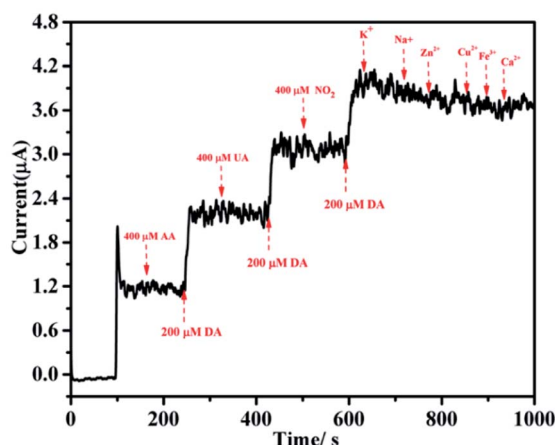


Fig. 10 (A)  $i$ - $t$  curve of DA in 0.1 M PBS buffer solution by the poly(-EDOT-MeSH)/Au (30 wt%) modified electrode; (B) linear standard curve of the modified electrode.

addition of 200  $\mu\text{M}$  DA, we observed a change in peak current intensity. It can be seen from the figure that the peak current intensity of DA was almost unchanged regardless of the addition of 2 times AA, UA and UA. In addition to interference by these three substances, the interference from common inorganic ions on the modified electrode was also tested. A change in current peak intensity was observed after continuously adding  $\text{K}^+$ ,  $\text{Na}^+$ ,  $\text{Ca}^{2+}$ ,  $\text{Zn}^{2+}$ , and  $\text{Fe}^{3+}$  at a concentration 10 times higher than that of DA. As shown, the addition of these inorganic ions has almost no effect on the peak current intensity of DA. From the above results, it can be seen that whether it is AA, UA,  $\text{NO}_2^-$  or common inorganic ions that often coexist with DA, there is no interference with the catalytic performance of the poly(EDOT-MeSH)/Au (30 wt%) modified electrode.

## 4. Conclusion

Thiol-functionalized poly(3,4-ethylenedioxythiophene)/gold composites (poly(EDOTMeSH)/Au) were prepared by a simple one-pot *in situ* polymerization method. The results show that the Au nanoparticles are uniformly supported on the inner and outer surfaces of the polymer by the S-Au bond during the polymerization. Spherical morphology and high electrocatalytic activities of the composite can be achieved by adjusting the content of  $\text{HAuCl}_4$ , as well controlling the size of the Au NPs on the polymers. In addition, strong bonding between Au and the thiol group can accelerate the electron kinetics of the composite modified materials, which gives the composites a high detection limit and selectivity.

## Conflicts of interest

There are no conflicts to declare.

## Acknowledgements

The authors are grateful to the Technology Science and Research Foundation of Xinjiang Institute of Engineering (No. 2020xgy062302) and the National Natural Science Foundation of China (No. 21764014).

## Notes and references

- 1 L. Z. Jing Sui, J. Travas-Sejdic and P. A. Kilmartin, *Macromol. Symp.*, 2010, **290**, 107–114.
- 2 Q. Jiang, D. Y. Xie, G. G. Fu, B. Huang, X. F. Zhao and Y. Zhao, *Mater. Sci. Forum*, 2011, **687**, 61–64.
- 3 Y. F. Zhu, Q. Q. Ni, Y. Q. Fu and T. Natsuki, *J. Nanopart. Res.*, 2013, **15**, 1–11.
- 4 W. Zhou, Y. Yu, C. Hao, F. J. Disalvo and H. D. Abrua, *J. Am. Chem. Soc.*, 2013, **135**, 16736–16743.
- 5 W. Li, Q. Zhang, G. Zheng, Z. W. Seh, H. Yao and Y. Cui, *Nano Lett.*, 2013, **13**, 5534–5540.
- 6 G. Duan, F. Lv, W. Cai, Y. Luo, Y. Li and G. Liu, *Langmuir*, 2010, **26**, 6295–6302.
- 7 A. Phongphut, C. Sriprachubwong, A. Wisitsoraat, A. Tuantranont, S. Prichanont and P. Sritongkham, *Sensor. Actuator. B Chem.*, 2013, **178**, 501–507.
- 8 W. Li, G. Zheng, Y. Yuan, W. S. Zhi and C. Yi, *Proc. Natl. Acad. Sci. U.S.A.*, 2013, **110**, 7148–7153.
- 9 Y. Xia, W. Min and L. Yun, *Synth. Met.*, 2009, **159**, 372–376.
- 10 L. Wu, W. Si, Y. Xu, Z. Gu and Q. Hao, *Microchim. Acta*, 2014, **181**, 707–722.
- 11 L. Yang, N. Huang, Q. Lu, M. Liu, H. Li, Y. Zhang and S. Yao, *Anal. Chim. Acta*, 2016, **903**, 69–80.
- 12 A. Ali, T. Abdiryim, X. Huang, R. Jamal and S. Rena, *J. Electrochem. Soc.*, 2018, **165**, B335–B343.
- 13 A. Ali, R. Jamal, T. Abdiryim and X. Huang, *J. Electroanal. Chem.*, 2017, **787**, 110–117.
- 14 Y. Zhang, M. Xin, W. Lin, Z. Yu, J. Peng, K. Xu and M. Chen, *Synth. Met.*, 2014, **193**, 8–16.
- 15 S. Harish, J. Mathiyarasu and K. Phani, *Mater. Res. Bull.*, 2009, **44**, 1828–1833.
- 16 Y. Xu, A. Q. Zhong, Z. D. He, A. Q. Zhon and K. Huang, *Microporous Mesoporous Mater.*, 2016, **229**, 1–7.
- 17 E. Pensa, E. Cortés, G. Corthey, P. Carro, C. Vericat, M. H. Fonticelli, G. Benítez, A. A. Rubert and R. C. Salvarezza, *Acc. Chem. Res.*, 2012, **45**, 1183.
- 18 W. K. Han, G. H. Hwang, S. J. Hong, H. H. An, C. S. Yoon, J. H. Kim, M. J. Lee, G. Hong, K. S. Park and S. G. Kang, *Appl. Surf. Sci.*, 2010, **256**, 2649–2653.
- 19 H. Tsunoyama, N. Ichikuni, H. Sakurai and T. Tsukuda, *J. Am. Chem. Soc.*, 2009, **131**, 7086–7093.
- 20 Z. Liu, J. Xu, R. Yue, T. Yang and L. Gao, *Electrochim. Acta*, 2016, 1–12.
- 21 Y. Zuo, J. Xu, F. Jiang, X. Duan, L. Lu, G. Ye, C. Li and Y. Yu, *J. Electroanal. Chem.*, 2017, **794**, 71–77.

